Combined density functional and dynamical cluster quantum Monte Carlo calculations of the three-band Hubbard model for hole-doped cuprate superconductors

P. R. C. Kent,[1] T. Saha-Dasgupta,[2] O. Jepsen,[3] O. K. Andersen,[3] A. Macridin,[4] T. A. Maier,[1] M. Jarrell,[4] and T. C. Schulthess[1]
[1]*Center for Nanophase Materials Sciences, Oak Ridge National Laboratory, Oak Ridge, Tennessee 37831, USA*
[2]*S. N. Bose National Centre for Basic Sciences, Kolkata 700 098, India*
[3]*Max-Planck-Institut für Festkörperforschung, D-70506 Stuttgart, Germany*
[4]*Department of Physics, University of Cincinnati, Cincinnati, Ohio 45221, USA*

Using a combined local density functional theory (DFT-LDA) and quantum Monte Carlo (QMC) dynamic cluster approximation approach, the parameter dependence of the superconducting transition temperature T_c of several single-layer hole-doped cuprate superconductors with experimentally very different $T_{c\,\max}$ is investigated. The parameters of two different three-band Hubbard models are obtained using the LDA and the downfolding Nth-order muffin-tin orbital technique with $N=0$ and 1, respectively. QMC calculations on four-site clusters show that the d-wave transition temperature T_c depends sensitively on the parameters. While the $N=1$ MTO basis set which reproduces all three $pd\sigma$ bands leads to a d-wave transition, the $N=0$ set which merely reproduces the LDA Fermi surface and velocities does not.

I. INTRODUCTION

Despite intense experimental and theoretical efforts, an understanding of high-temperature superconductivity (HTSC) in hole-doped cuprate materials is elusive. While the materials are increasingly well characterized,[1] a firm theoretical linking of the superconducting transition temperature T_c to details of the underlying atomistic and electronic structures remains a grand challenge in condensed-matter theory.

Recent advances in quantum cluster theories have given insight into the two-dimensional (2D) one-band Hubbard model, the most commonly adopted many-electron model for these materials. At low temperatures and appropriate hole concentrations, the model develops the requisite strong $d_{x^2-y^2}$ order and superconducting ground state[2–4] due to magnetically driven pairing.[5–8] If this model captures sufficient physics to describe real materials, the magnetic interactions and resultant T_c should be moderated by details of the actual materials and their electronic structures.

In parallel with the Hubbard investigations, the electronic structure of HTSCs has been extensively studied using density functional theory[9] (DFT). Although structural properties are well reproduced, conventional DFT-local density approximation (LDA) calculations fail to describe the undoped insulating ground state.[10–13] Nevertheless, DFT calculations agree on a universal electronic structure in these materials: the low-energy electronic degrees of freedom are primarily the $pd\sigma$ antibonding O p and Cu $d_{x^2-y^2}$ orbitals in the CuO_2 layer, and these bands have been parameterized.[14–17] For all optimally and overdoped materials, the Fermi surfaces (FSs) measured by angle-resolved photoemission[18] (ARPES) agree surprisingly well with detailed LDA predictions. Even the existence and distinct in-plane dispersion of the splitting between the two FS sheets in bilayered cuprates[14] and the k_z dispersion in body-centered tetragonal single-layered materials,[19] have recently been experimentally confirmed.[18,20] Finally, the LDA conduction-band parameter $r\sim -t'/t$,[14] which gives the material dependence of the FS shape and has the same origin as $t_\perp(\mathbf{k}_\parallel)$, has been found to correlate positively with $T_{c\,\max}$,[19] but causal links have not been established.

In this paper we combine LDA-DFT calculations of the cuprates with quantum cluster calculations of the transition temperatures T_c of the 2D Hubbard model. We study the three- rather than the one-band model because the most localized Cu $d_{x^2-y^2}$-like orbital describing the LDA conduction band is so extended,[21] that using merely the on-site Coulomb repulsion in a one-band model is not justified. However, including also the $O_x p_x$, and $O_y p_y$ orbitals in the basis set, localizes the Cu $d_{x^2-y^2}$ orbital to the extent that the corresponding three-band Hubbard Hamiltonian appears to be a valid model. DFT calculations are used to consistently obtain the parameters for the five single-layer materials $HgBa_2CuO_4$, $Tl_2Ba_2CuO_6$, TlBa $LaCuO_5$, La_2CuO_4, and $Ca_2CuO_2Cl_2$, for which $T_{c\,\max}=90$, 85, 52, 40, and 26 K, respectively. To determine T_c we use the dynamic cluster approximation (DCA) with a finite-temperature quantum Monte Carlo (QMC) cluster solver[22–24] and the previously calculated DFT parameters.[25] In principle, these calculations use no experimental input and are therefore a stringent test of both the density functional and quantum cluster methods, as well as the form of the underlying model. As the first study of this type, we aim to address the following questions: (1) What is the magnitude of T_c variation in the Hubbard model following the LDA+DCA scheme, and is this variation realistic? (2) Are there parameters found by LDA-DFT beyond those typically considered in Hubbard-like schemes that are particularly important for determining T_c in these materials?[26]

II. DENSITY FUNCTIONAL CALCULATIONS

We approximate the LDA potential for the stoichiometric (undoped) cuprates by a superposition of spherically symmetric, overlapping potential wells and then construct the basis set of three orbitals per cell by downfolding within

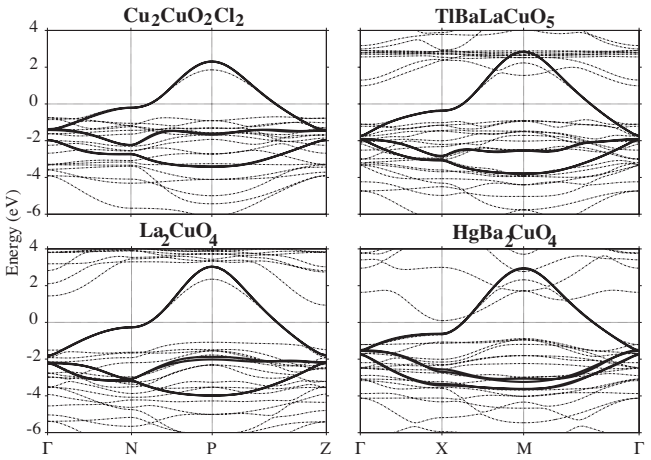

FIG. 1. Comparison of the downfolded N=0 MTO three-band (bold) and complete LDA band structures (dashed) of four undoped single-layer HTSC materials. The zero of energy is the Fermi level.

multiple-scattering theory at the LDA Fermi energy, ϵ_F. Such an orbital is constructed to have the following properties: (1) It solves Schrödinger's differential equation at ϵ_F throughout the solid, i.e., in all partial-wave channels, except for a kink at the muffin-tin (MT) spheres in the Cu $d_{x^2-y^2}$, O$_x p_x$, and O$_y p_y$ channels. (2) It has *no* Cu $d_{x^2-y^2}$, O$_x p_x$, or O$_y p_y$ character inside any MT sphere other than the one in which the orbital is centered and has its own character. Hence, the orbital is chosen to vanish (with a kink) in the channels of the other orbitals, and this makes it maximally localized. Pictures are presented in Ref. 25. This basis set of kinked partial waves[21] provides Bloch solutions of Schrödinger's equation with errors proportional to $\varepsilon(\mathbf{k})-\epsilon_F$, and energy bands with errors proportional to $[\varepsilon(\mathbf{k})-\epsilon_F]^2$ due to the variational principle. The LDA FS and velocities are thus given correctly, as can clearly be seen from Fig. 1. For the solutions of Schrödinger's equation at ϵ_F, the kinks cancel out.

Instead of using kinked partial waves at ϵ_F as basis functions, we could have constructed Nth-order muffin-tin orbitals[21] (N MTOs) which for a *mesh* of energies, $\epsilon_0, \ldots, \epsilon_N$, yield wave functions with errors proportional to $[\varepsilon(\mathbf{k})-\epsilon_0]..[\varepsilon(\mathbf{k})-\epsilon_N]$. In that way, the three bands can be made to reproduce the LDA bands over a wider energy range, specifically the range set by $U_{dd}\approx 10$ eV. In addition to the above-mentioned N=0 set, we shall also consider an N=1 set with the second energy, ϵ_1, chosen near the bottom of the $pd\sigma$ bonding band, i.e., 7–8 eV below $\epsilon_0 \equiv \epsilon_F$. As seen in Fig. 3, this basis set accounts for the LDA $pd\sigma$ bonding, nonbonding, and antibonding bands, at the same time as it reproduces the LDA FS and velocities. However, its orbitals are slightly less localized.

Symmetrical orthormalization of the three N MTOs finally yields the orbital representation in which $\hat{H}$ is expressed. The on-site elements of H_{LDA} are the orbital energies, $\epsilon_\alpha^{\mathrm{LDA}}$, and the off-site elements are the integrals for hopping, $t_{\alpha ij}^{\beta lm}$, between orbital α on site ij and orbital β on site lm in the same CuO$_2$ layer. Interlayer hopping is neglected in this study. The site indices for the d orbital are integers, since it is on a cubic lattice, while those for the x (y) orbital are $\frac{1}{2}0$ ($0\frac{1}{2}$) plus integers. The orbitals, centered on the Cu and O sites, are orthonormal and real by construction. On-site energies and hopping integrals are, therefore, real and symmetric. The Fourier components of $H(\mathbf{k})_{\mathrm{LDA}}$ are, for example $H_{dd}(\mathbf{k})=\epsilon_d+2t_{d00}^{d10}(\cos k_x+\cos k_y)+4t_{d00}^{d11}\cos k_x \cos k_y+\ldots$. Table I gives the short notation used for the hopping integrals.

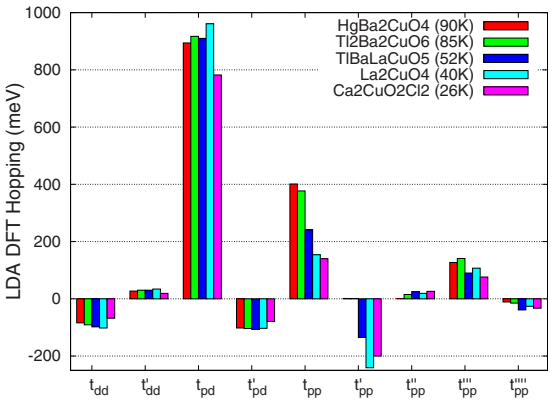

FIG. 2. (Color online) Calculated in-layer hoppings for five single-layer cuprates for N=0. The materials are ordered by $T_{c\,\max}$.

The values of the hopping integrals for the N=0 basis set are shown in Fig. 2. They have reasonably short range and are dominated by the usual t_{pd} and t_{pp}. The values ~0.9 eV of t_{pd} are considerably smaller than the conventional value 1.5 eV (Ref. 14–17) describing the width $\sim 4\sqrt{2}t_{pd}$ ~8.5 eV of the $pd\sigma$ antibonding *and* bonding bands. Whereas t_{pd} and most other hopping integrals are seen to be fairly independent of the material (only the one with apical Cl is a bit smaller), t_{pp} is *not*; it increases with the observed $T_{c\,\max}$. This is the conduction-band trend found previously[19] and explained as p_x to p_y hopping via a high-energy (ϵ_s), Cu-centered *axial* hybrid consisting of Cu 4s, Cu $3d_{3z^2-1}$, apical oxygen $2p_z$, and axial cation orbitals, all stacked perpendicular to the layer. If the energy of this axial orbital is increased (e.g., by moving apical oxygen closer to Cu), $t_{pp} \sim \frac{t_{sp}^2}{\epsilon_s-\epsilon_F}$ decreases.[14] Within that axial model, $t'_{pp}=t_{pp}$, but Fig. 2 shows that this is not true: t_{pp} vanishes for the two high-T_c cuprates, and for the three low-T_c cuprates, the sign of t'_{pp} is opposite to that of t_{pp}. The main reason is that hopping via the in-layer (and therefore material independent) Cu $4p_x$ orbital contributes to t_{pp}, but not to t_{pp}, and opposes the hopping via the axial orbital.[25] Also material-independent hopping via O$_y p_x$ orbitals influences t_{pp}, and causes a sizeable t'''_{pp}. So t_{pp} and t'_{pp} exhibit the material's trend. Finally, t_{dd}

TABLE I. Relationship between site index and short-form notation used for hopping integrals

t_{d000}^{d100}	t_{d000}^{d110}	$t_{d000}^{x1/200}$	$t_{d000}^{x1/210}$	$t_{d000}^{x3/200}$	$t_{d000}^{x3/210}$	$t_{x\frac{-1}{2}00}^{y01/20}$	$t_{x\frac{-1}{2}00}^{x1/200}$	$t_{x1/200}^{x1/210}$	$t_{x-1/200}^{x1/210}$	$t_{x-1/200}^{y11/20}=t_{x-1/200}^{y03/20}$
t_{dd}	t_{dd}	t_{pd}	t_{pd}	t''_{pd}	t'''_{pd}	t_{pp}^2	t_{pp}^2	t''_{pp}	t'''_{pp}	t''''_{pp}

proceeds mainly via the diffuse O_x $3d_{3x^2-1}$ orbital, lying 50 eV above ϵ_F, and t'_{pd} proceeds mainly via polarization of the cation. In summary, (1) diffuse high-energy (ϵ_γ) orbitals make sizeable contributions $\propto t^2_{\alpha\gamma}/(\epsilon_F-\epsilon_\gamma)$ to the LDA hopping integrals and (2) the energy ϵ_s of the axial orbital, here downfolded into the tails of the oxygen orbitals, is the essential material-dependent parameter.

The Cu on-site Coulomb energy is $U_{dd}\approx 9.5$ eV in all five cuprates as found by constrained LDA (Ref. 27) calculations with the LMTO-ASA method. The radius of the Cu sphere is adjusted to 1.32 Å, such that the d character in the upper half of the LDA conduction band, the d hole-count $h_d^{\rm LDA}$, is the same as that obtained from the three-band $H_{\rm LDA}$. This ensures that the Cu $d_{x^2-y^2}$ partial wave truncated outside the atomic sphere is similar to the Cu $d_{x^2-y^2}$ partner of the three-orbital N MTO set. For the four cuprates with apical oxygen, we find: $h_d^{\rm LDA}=0.46$ and for the diagonal elements of $H_{\rm LDA}$: $\epsilon_d^{\rm LDA}(h_d)-\epsilon_p\approx 0.45$ eV. Since correlation effects are already taken into account at the mean-field level in the LDA, we must include a double-counting correction proportional to the deviation, $h_d^{\rm LDA}-\frac{1}{2}$, of the d hole count from that ($\frac{1}{2}$) of the $d^9\rightarrow d^{10}$ transition state. The corrected orbital-energy difference is then: $\Delta\equiv e_p-e_d=\epsilon_d+U_{dd}-\epsilon_p=\epsilon_d^{\rm LDA}(h_d^{\rm LDA})-\epsilon_p+(h_d^{\rm LDA}-\frac{1}{2})U_{dd}\approx 0.0$ eV, where e refers to the hole and ϵ to the electron representation. The commonly assumed value is, however, $\Delta\sim 3$ eV.[15–17] Previous constrained LDA calculations for La_2CuO_4 (Refs. 15 and 16) gave 3 eV because they used the LMTO-ASA total d electron count of 9.24 to deduce $h_d^{\rm LDA}=0.76$, and then found the double-counting correction to be ~2.5 eV. However, integrating to the top of the conduction band, we find not 10, but 9.70 d electrons, which is consistent with $h_d^{\rm LDA}=0.46$.[28]

Unfortunately, current many-body treatments fail to reproduce the insulating behavior at half filling, unless Δ exceeds 3 eV, and this is commonly felt to be unacceptable. We therefore empirically set $\Delta=3.25$ eV in $H_{\rm LDA}$, i.e., we increased $\epsilon_d^{\rm LDA}-\epsilon_p$ by 3.25 eV, but kept our hopping integrals unchanged.[29] This does not completely ruin the agreement between the experimental and LDA FS shapes, but it weakens the trend: For $Tl_2Ba_2CuO_6$ the effective $-t'/t$ is reduced from 0.33 (Ref. 19) to 0.22, with the experimental[20] value being 0.28, while for La_2CuO_4 the reduction is merely from 0.17 to 0.16. In all five cases, the Δ shift causes a 20% reduction of the effective conduction bandwidth $8t$.

With the $N=1$ basis set, which describes the three LDA $pd\sigma$ bands over the energy range U_{dd}, rather than merely the antibonding band near the LDA Fermi level (see Figs. 1 and 3), the values of the hopping integrals for $HgBa_2CuO_4$ (90 K) and La_2CuO_4 (40 K) are as shown in Fig. 4. Now t_{pd} is increased to values much closer to the conventional ones[14–17] and t_{pp} is increased to 0.90 eV. By having to span a wider energy range, the $N=1$ orbitals are somewhat less localized, and consequently have somewhat longer-ranged hoppings, than the $N=0$ orbitals. This also masks the material's trend in individual hopping integrals, although it is of course present in the shape of the antibonding band near ϵ_F. Now $\epsilon_d^{\rm LDA}-\epsilon_p=0.67$ and 0.95 eV for $HgBa_2CuO_4$ (90 K) and La_2CuO_4, respectively, but for the reason mentioned above, we shall set Δ to 3.25 eV.

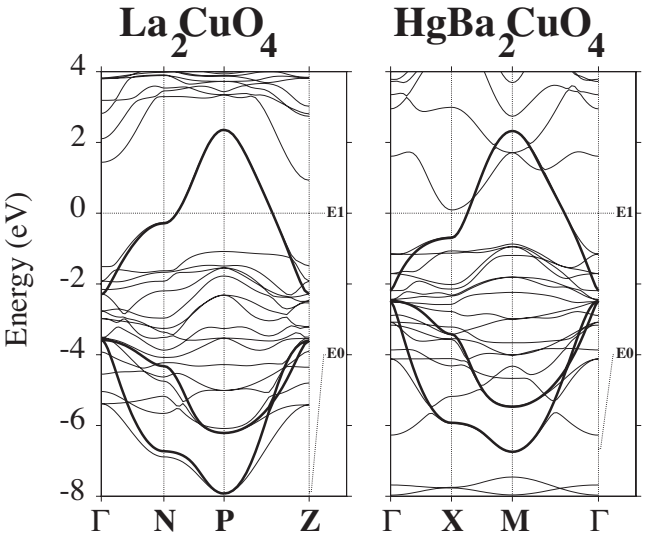

FIG. 3. Comparison of the downfolded $N=1$ three-band (bold) and complete LDA band structures (dashed) of the single-layer HTSC materials $HgBa_2CuO_4$ and La_2CuO_4. The zero of energy is the Fermi level.

III. DYNAMIC CLUSTER APPROXIMATION CALCULATIONS

To solve the three-band Hubbard Hamiltonian $\hat{H}$, we use the DCA (Refs. 23 and 24) (for a review, see Ref. 30). In this method we map the lattice model onto a periodic cluster of size $L_c\times L_c$, embedded into a self-consistently determined mean-field background. Correlations up to a range $\sim L_c$ are treated explicitly while longer-ranged correlations are treated at a mean-field level. We solve the cluster problem using QMC,[22] which does not introduce further significant approximations. Calculations on large clusters at low temperatures become prohibitively (exponentially) expensive due to the QMC Fermion sign problem. T_c is determined via the diverging d-wave pair-field susceptibility obtained over a series of calculations at progressively lower temperatures. We check for earlier divergences in other angular momentum channels.

Due to the large computational cost of a parametric study using QMC, we have performed calculations on four-site

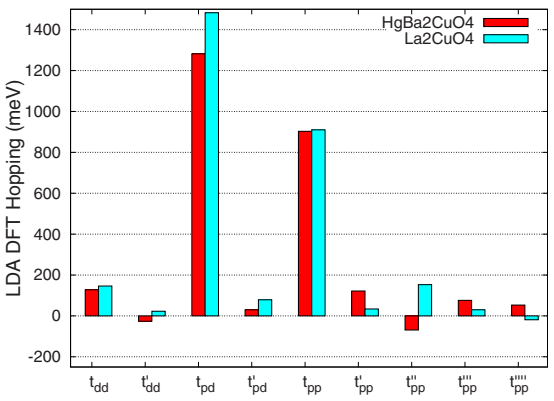

FIG. 4. (Color online) Comparison of calculated in-layer hoppings for two single-layer cuprates for $N=0$ and $N=1$ (see text).

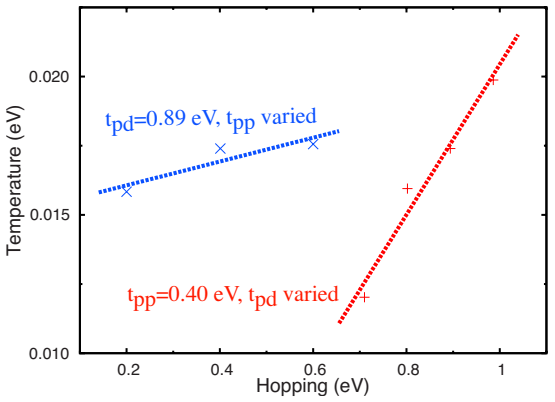

FIG. 5. (Color online) Calculated transition temperatures T_c for the three-band $t_{pd}-t_{pp}$ model (see text). The temperature variation is shown for variations in t_{pp} with t_{pd}, held fixed (blue crosses), and vise versa (red plusses). The guide lines are a linear fit.

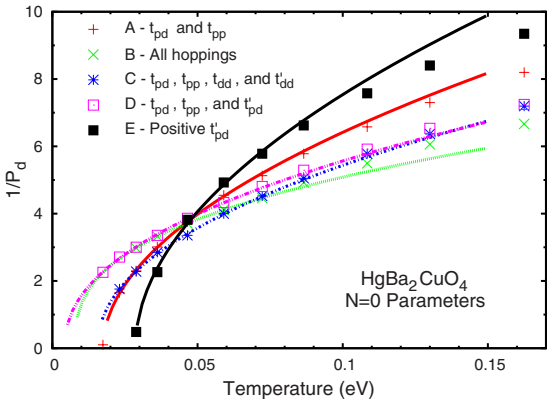

FIG. 6. (Color online) Inverse d-wave pair-field susceptibility (P_d^{-1}) as a function of temperature for different hopping-parameter sets calculated from $HgBa_2CuO_4$ with $N=0$ (see text). The lines are power-law fits to the lowest five points in each series.

clusters ($L_c=2$) at 15% hole doping, which is near optimal in real materials. The four-site cluster is the smallest for which a d-wave order parameter is allowed topologically, and corresponds to a mean-field result.[2] Single-band calculations on four-site clusters have shown that the phase diagram of these clusters shows general agreement with HTSC.[30] Converged calculations on clusters of up to 26 sites—for a single set of parameters—find that T_c of four-site clusters is *over* estimated by a factor ~ 2,[2] i.e., the small clusters exhibit larger pairing correlations. Hence, the presence of d-wave order in four-site clusters at low temperature does not confirm the existence of such order in larger clusters, while the absence of d-wave order strongly indicates an absence of this order in the thermodynamic limit. In all of our DCA calculations, we consistently used the calculated hoppings t and not, for example, the original LDA dispersion.

To establish the existence of a variation in T_c in the three-band model, we performed an initial parametric study using only the nearest-neighbor hopping integrals t_{pd} and t_{pp}. Leaving one of these fixed at the value calculated with the $N=0$ basis set for $HgBa_2CuO_4$, our highest $T_{c\,\max}$ material, we varied the other. As shown in Fig. 5, a d-wave transition was obtained over the entire range of parameters studied. Increasing either parameter increased T_c, and $dT_c/dt_{pd} \sim 6.3 \times dT_c/dt_{pp}$. The increase of T_c with increased t_{pd} may be understood in terms of changes to the fundamental energy scale. Within the range of studied materials, however, the calculated variation of t_{pd} is rather insignificant due to very similar Cu-O bond lengths while t_{pp} varies systematically, with larger values corresponding to materials with larger $T_{c\,\max}$, a trend reproduced by our QMC calculations.

In Fig. 6 we show the calculated inverse d pair-field susceptibility as a function of temperature for $HgBa_2CuO_4$ with the $N=0$ basis set when all hoppings are included, as well as subsets of hoppings. Compared to the inverse susceptibility of the $t_{pd}-t_{pp}$ only calculation (A), which yields a moderate $T_c \sim 17$ meV, when including all the hoppings (B), the inverse susceptibility is reduced at high temperatures, but reduces less quickly at lower temperatures. Therefore, any transition for the true LDA $N=0$ hoppings must occur at much lower temperatures than for the $t_{pd}-t_{pp}$ only case. The d hole occupancy at low temperature is $h_d \sim 0.76$ compared to ~ 0.78 for the $t_{pd}-t_{pp}$ case. For the complete set (B), there appears to be no d-wave transition at moderate temperatures. Due to the increasing computational cost for lower temperatures, we cannot completely exclude the possibility of a very low-temperature transition, but it is certain that any T_c is significantly reduced from the simpler $t_{pd}-t_{pp}$ only case. When calculations are performed for all five materials (not shown), we also find no apparent d-wave transitions. These results demonstrate that, surprisingly, T_c of the three-band Hubbard model is a strong function of the hopping parameters beyond the nearest neighbors.

To investigate the cause of the T_c reduction, we systematically surveyed the effect of varying each hopping parameter to extract $dT_c/dt_{\alpha ij}^{\beta lm}$. In (C) we see that adding t_{dd} and t'_{dd} to t_{pd} and t_{pp} is not what suppresses T_c, but adding t_{pd} does, as seen in (D). Although all hopping parameters modify T_c, variation of t_{pd} changes T_c most dramatically. This hopping proceeds mainly via polarization of the cation and is -0.10 eV for all five materials. Changing the sign of t'_{pd}, but keeping all other hoppings realistic, even produces a significant enhancement of T_c as shown in (E). This artificial sign change profoundly changes the $U=0$ conduction band: the effective t decreases by a factor of 2 from the full LDA value, and $-t'/t$ decreases from 0.34 to 0, i.e., this change is opposite to the empirical trend.[19]

We now repeat the calculations using the $N=1$ basis set which reproduces all three LDA $pd\sigma$ bands over a range of 10 eV $\sim U_{dd}$ (see Figs. 3 and 4). The inverse d pair-field susceptibilities for $HgBa_2CuO_4$ are shown in Fig. 7. When all the hoppings are included (B), the susceptibility is increased at all temperatures compared to the $N=0$ case, and in contrast to the previous results, there does appear to be a d-wave transition at very low temperature. This result clearly demonstrates a strong sensitivity of the many-body results on details of the treatment of the LDA data and Hubbard Hamiltonian.

To further investigate the differences between the $N=0$ and $N=1$ parameter sets, we performed $N=1$ calculations including only t_{pp} and t_{pd}. From Fig. 7 we see that neglecting all hoppings except these two between nearest neighbors has

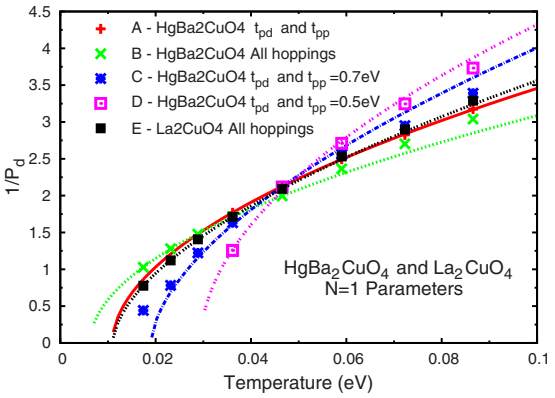

FIG. 7. (Color online) Inverse d-wave pair-field susceptibility (P_d^{-1}) as a function of temperature for different hopping-parameter sets calculated from $HgBa_2CuO_4$ and for La_2CuO_4 with $N=1$ (see text). The lines are power-law fits to the lowest five points in each series.

little effect on the susceptibility (A). This result is in marked contrast with the one for the $N=0$ set, where the removal of long-ranged terms, particularly t'_{pd}, significantly increased T_c. This is presumably connected with the fact that t'_{pd} changes sign when going from $N=0$ to $N=1$. We also show the effect of *decreasing* t_{pp} with $t_{pd}=1.28$ eV [(C) and (D)]: in contrast to results for $t_{pd}=0.89$ eV (Fig. 5) we find T_c to *increase*. This does not contradict the empirical trend that $T_{c\,\max}$ increases with t'/t because this does not translate into an increase with t_{pp} for the $N=1$ set. Comparisons of the inverse susceptibility for calculations performed with the full parameter sets for $HgBa_2CuO_4$ (B) and La_2CuO_4 (E) indicate that La_2CuO_4 will have the higher transition temperature, the reverse order compared to experiment.

As an additional independent test on the choice of downfolding method, we repeated the QMC calculations using $HgBa_2CuO_4$ hopping parameters determined by a Wannier-function projection method[31] which, like the $N=1$ set, reproduced all three $pd\sigma$ bands. Nevertheless, in this case we found *no* d-wave transition in the computationally accessible temperature range (a low-temperature transition cannot be ruled out).

The above results clearly demonstrate that the phase diagram of the three-band Hubbard model is quite sensitive to the choice of hopping integrals, even around the commonly accepted energy range of $t_{pd}\sim 1$ eV. Although a d-wave transition is found for the $N=1$ MTO basis set which reproduces all three $pd\sigma$ LDA bands as well as the LDA FS and velocities, no transition is found for slightly different choices of downfolding approach, e.g., for Wannier-function projection of the three bands or for the $N=0$ MTO basis which only reproduces the LDA FS and velocities. We have only investigated a single point on the phase diagram due to the computational expense and numerical difficulty of the current QMC and DCA techniques. Within the three-band Hamiltonian, refinement of the ill-determined $\Delta=e_p-e_d$ is clearly required, as well as investigation of the effect of different hoppings on the spectral properties. It is also highly desirable to investigate larger clusters as well as more complex Hamiltonians: for example, in LDA-DFT the $d_{3z^2-r^2}$ band lies close to the Fermi energy in some of the HTSC materials, suggesting that additional Cu degrees of freedom may be required. Unfortunately these investigations are currently precluded due to the computational cost and worsening Fermion sign problem; we hope they will be examined in future.

IV. CONCLUSIONS

In summary, we have obtained the parameters of three-band Hubbard models for a series of single-layer cuprate superconductors with varying $T_{c\,\max}$ from downfolding either to the LDA conduction band or to all three $pd\sigma$ bands. The transition temperature calculated using DCA-QMC on four-site clusters and increasing the small LDA value of e_p-e_d to 3.25 eV is a moderate to very strong function of the hopping parameters. Even small hopping integrals beyond the nearest-neighbors can have a marked effect on the transition temperatures. These parameters are sensitive to the choice of downfolding technique and effective degree of Wannier localization. The present calculations yields superconductivity for the NMTO basis set which reproduces all three $pd\sigma$ LDA bands, but not for the one which reproduces merely the LDA Fermi surface and velocities. We hope that our findings will motivate future investigations and methodological development of more robust approaches for constructing and/or for solving realistic models of the cuprate superconductors.

ACKNOWLEDGMENTS

We thank O. Gunnarsson, I. Dasgupta, J. P. Hague, and D. J. Scalapino for useful discussions, and W. Ku for providing alternative hopping parameters. T.S.D. and O.K.A. acknowledge the MPG-India partner group program. A portion of this research was conducted at the Center for Nanophase Materials Sciences at Oak Ridge National Laboratory, used computational resources of the Center for Computational Sciences, and was sponsored by the offices of Basic Energy Sciences and Advanced Scientific Computing Research, U.S. Department of Energy. A.M. and M.J. were supported by CMSN DOE Contract No. DE-FG02-04ER46129 and NSF Contract No. DMR-0312680.

[1] *Handbook of Superconducting Materials*, edited by D. A. Cardwell and D. S. Ginley (CRC, Boca Raton, FL, 2003).

[2] T. A. Maier, M. Jarrell, T. C. Schulthess, P. R. C. Kent, and J. B. White, Phys. Rev. Lett. **95**, 237001 (2005).

[3] D. Sénéchal, P.-L. Lavertu, M.-A. Marois, and A.-M. S. Tremblay, Phys. Rev. Lett. **94**, 156404 (2005).

[4] S. S. Kancharla, B. Kyung, D. Senechal, M. Civelli, M. Capone, G. Kotliar, and A.-M. S. Tremblay, Phys. Rev. B **77**, 184516 (2008).

[5] T. A. Maier, M. S. Jarrell, and D. J. Scalapino, Phys. Rev. Lett. **96**, 047005 (2006).

[6] T. A. Maier, M. Jarrell, and D. J. Scalapino, Phys. Rev. B **74**,

094513 (2006).
[7] T. A. Maier, M. Jarrell, and D. J. Scalapino, Phys. Rev. B **75**, 134519 (2007).
[8] M. Aichhorn, E. Arrigoni, M. Potthoff, and W. Hanke, Phys. Rev. B **74**, 024508 (2006).
[9] W. E. Pickett, Rev. Mod. Phys. **61**, 433 (1989).
[10] J. Zaanen, O. Jepsen, O. Gunnarsson, A. T. Paxton, O. K. Andersen, and A. Svane, Physica C **153-155**, 1636 (1988).
[11] V. I. Anisimov, J. Zaanen, and O. K. Andersen, Phys. Rev. B **44**, 943 (1991).
[12] A. Svane, Phys. Rev. Lett. **68**, 1900 (1992).
[13] W. M. Temmerman, Z. Szotek, and H. Winter, Phys. Rev. B **47**, 11533 (1993).
[14] O. K. Andersen, A. I. Liechtenstein, O. Jepsen, and F. Paulsen, J. Phys. Chem. Solids **56**, 1573 (1995).
[15] A. K. McMahan, J. F. Annett, and R. M. Martin, Phys. Rev. B **42**, 6268 (1990).
[16] M. S. Hybertsen, M. Schluter, and N. E. Christensen, Phys. Rev. B **39**, 9028 (1989).
[17] F. Mila, Phys. Rev. B **38**, 11358 (1988).
[18] A. Damascelli, Z. Hussain, and Z. Shen, Rev. Mod. Phys. **75**, 473 (2003).
[19] E. Pavarini, I. Dasgupta, T. Saha-Dasgupta, O. Jepsen, and O. K. Andersen, Phys. Rev. Lett. **87**, 047003 (2001).
[20] N. E. Hussey, M. Abdel-Jawad, A. Carrington, A. P. Mackenzie, and L. Balicas, Nature (London) **425**, 814 (2003).
[21] O. K. Andersen and T. Saha-Dasgupta, Phys. Rev. B **62**, R16219 (2000).
[22] M. Jarrell, T. Maier, C. Huscroft, and S. Moukouri, Phys. Rev. B **64**, 195130 (2001).
[23] M. H. Hettler, A. N. Tahvildar-Zadeh, M. Jarrell, T. Pruschke, and H. R. Krishnamurthy, Phys. Rev. B **58**, R7475 (1998).
[24] M. H. Hettler, M. Mukherjee, M. Jarrell, and H. R. Krishnamurthy, Phys. Rev. B **61**, 12739 (2000).
[25] T. Saha-Dasgupta, J. Nuss, O. Jepsen, and O. K. Andersen (unpublished).
[26] Q. Yin, A. Gordienko, X. Wan, and S. Y. Savrasov, Phys. Rev. Lett. **100**, 066406 (2008).
[27] O. Gunnarsson, O. K. Andersen, O. Jepsen, and J. Zaanen, Phys. Rev. B **39**, 1708 (1989).
[28] The 0.3 d electron missing is d_{3z^2-1}, which extends in the z direction, beyond the sphere. In our three-band model, this orbital is downfolded into the tails of the Op orbitals (Ref. 25).
[29] Using a two-hopping parameter model, we find T_c variatons of 1% for $e_p - e_d = 3.5$ and 4.79 eV.
[30] T. Maier, M. Jarrell, T. Pruschke, and M. H. Hettler, Rev. Mod. Phys. **77**, 1027 (2005).
[31] W. Ku, H. Rosner, W. E. Pickett, and R. T. Scalettar, Phys. Rev. Lett. **89**, 167204 (2002).